Article

Cell Reports

MEIS2 Is an Oncogenic Partner in AML1-ETO-Positive AML

Graphical Abstract

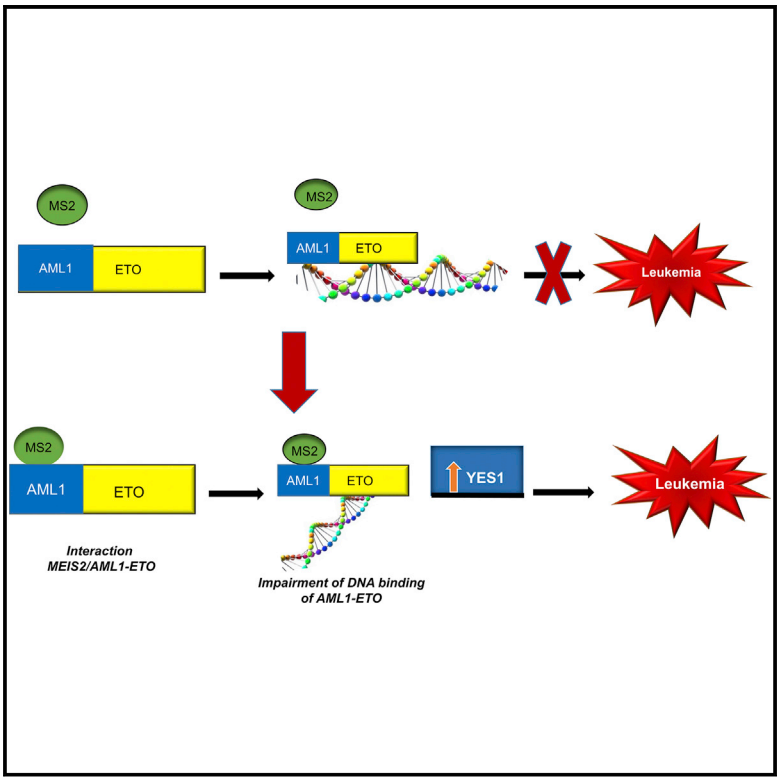

Authors

Naidu M. Vegi, Josef Klappacher, Franz Oswald, ..., Hendrik G. Stunnenberg, Michaela Feuring-Buske, Christian Buske

Correspondence

christian.buske@uni-ulm.de

In Brief

AML1-ETO is the most frequent fusion gene in human acute myeloid leukemia, but it is difficult to target therapeutically. Vegi at al. find that the homeobox gene MEIS2 is an oncogenic partner in *AML1-ETO*-positive AML. MEIS2 alters the DNA binding properties of AML1-ETO, resulting in reduced transcriptional repression of *YES1*, which is thus a possible therapeutic target.

Highlights

- *MEIS2* is aberrantly expressed in *AML1-ETO* AML
- Co-expression of MEIS2 with AML1-ETO induces AML in a murine model
- MEIS2 strongly binds to AML1-ETO
- MEIS2 increases YES1 expression by impairing AML1-ETO DNA binding

Accession Numbers

GSE81174
GSE81321
GSE81328
GSE81329

Vegi et al., 2016, Cell Reports *16*, 498–507
July 12, 2016
http://dx.doi.org/10.1016/j.celrep.2016.05.094

OPEN ACCESS
CellPress

Cell Reports
Article

MEIS2 Is an Oncogenic Partner in AML1-ETO-Positive AML

Naidu M. Vegi,[1] Josef Klappacher,[1] Franz Oswald,[2] Medhanie A. Mulaw,[1] Amit Mandoli,[3] Verena N. Thiel,[2] Shiva Bamezai,[1] Kristin Feder,[1] Joost H.A. Martens,[3] Vijay P.S. Rawat,[1] Tamoghna Mandal,[1] Leticia Quintanilla-Martinez,[4] Karsten Spiekermann,[5] Wolfgang Hiddemann,[5] Konstanze Döhner,[6] Hartmut Döhner,[6] Hendrik G. Stunnenberg,[3] Michaela Feuring-Buske,[6] and Christian Buske[1,7,*]

[1]Institute of Experimental Cancer Research, CCC and University Hospital of Ulm, 89081 Ulm, Germany
[2]Department of Internal Medicine I, Center for Internal Medicine, University Medical Center Ulm, Albert-Einstein-Allee 23, 89081 Ulm, Germany
[3]Department of Molecular Biology, Faculty of Science, Nijmegen Centre for Molecular Life Sciences, Radboud University, 6500HB Nijmegen, the Netherlands
[4]Institute of Pathology and Neuropathology, Eberhard Karls University of Tübingen and Comprehensive Cancer Center, University Hospital Tübingen, Liebermeisterstrasse 8, 72076 Tübingen, Germany
[5]Department of Internal Medicine III, University Hospital Grosshadern, Ludwig-Maximilians-University (LMU), 81377 Munich, Germany
[6]Department of Internal Medicine III, University Hospital Ulm, 89081 Ulm, Germany
[7]Core Facility Genomics, Medical Faculty Ulm, Ulm University, 89081 Ulm, Germany
*Correspondence: christian.buske@uni-ulm.de
http://dx.doi.org/10.1016/j.celrep.2016.05.094

SUMMARY

Homeobox genes are known to be key factors in leukemogenesis. Although the TALE family homeodomain factor *Meis1* has been linked to malignancy, a role for *MEIS2* is less clear. Here, we demonstrate that *MEIS2* is expressed at high levels in patients with AML1-ETO-positive acute myeloid leukemia and that growth of AML1-ETO-positive leukemia depends on MEIS2 expression. In mice, MEIS2 collaborates with AML1-ETO to induce acute myeloid leukemia. MEIS2 binds strongly to the Runt domain of AML1-ETO, indicating a direct interaction between these transcription factors. High expression of MEIS2 impairs repressive DNA binding of AML1-ETO, inducing increased expression of genes such as the druggable proto-oncogene *YES1*. Collectively, these data describe a pivotal role for MEIS2 in AML1-ETO-induced leukemia.

INTRODUCTION

Aberrant expression of clustered homeobox genes, or *HOX* genes, is a molecular hallmark of acute myeloid leukemia (AML), and many experimental studies have proven that dysregulated expression of this highly conserved family of transcription factors is a key factor in leukemia development (Alharbi et al., 2013; Argiropoulos et al., 2007; Jung et al., 2015; McGonigle et al., 2008; Spencer et al., 2015). Besides HOX genes, non-clustered homeobox genes, such as the ParaHox gene *CDX2,* have been shown to play an essential role in leukemogenesis (Faber et al., 2013; Lengerke and Daley, 2012; Rawat et al., 2012), as have members of the three-amino-acid-loop extension (TALE) superfamily, *MEIS1* and *PBX1* (Argiropoulos et al., 2007). The TALE superfamily is characterized by three highly conserved additional residues, proline-tyrosine-proline, in the first loop region of the homeodomain (Bürglin, 1997). So far, three functional *Meis* genes have been identified (*Meis1*, *Meis2*, and *Meis3*). MEIS1 and MEIS2 show 82% homology at the amino acid level. Homology is particularly high within the homeodomain and in a second conserved domain, the homothorax homology domain (Hth) (Moens and Selleri, 2006). There is a rich body of evidence arguing that Meis1 plays a pivotal role in normal and malignant hematopoiesis. Murine transplantation models clearly showed that Meis1 collaborates with native Hox genes such as HoxA9 and HoxA10 and multiple NUP98-HOX fusion genes in inducing AML (Kroon et al., 1998; Pineault et al., 2003; Thorsteinsdottir et al., 2001). Furthermore, MEIS1 and multiple HOX genes are aberrantly expressed in a variety of human AML genotypes such as NPM1 mutated cytogenetically normal (CN)-AML or AML with complex karyotype (Kawagoe et al., 1999; Rawat et al., 2008). Interestingly, to date, MEIS1 is the only MEIS family member to be implicated in normal or leukemic hematopoiesis. In this report, we characterize *MEIS2* as a potent oncogene in AML1-ETO (AE)-positive AML.

RESULTS

The Homeobox Gene *MEIS2* Is Aberrantly Expressed in Patients with AE-Positive AML

Because there are few reports on the expression and function of *MEIS2* in AML, expression of this gene was evaluated in a large cohort of patients with AML and normal $CD34^+$ bone marrow (BM) cells by real-time qPCR (Table S1). Strikingly, *MEIS2* expression in AE-positive AML was significantly higher than in *PML-RARA* and *inv(16)* positive cases ($n = 11$) ($p < 0.0001$) (Figure 1A). There was also high expression in CN-AML, independent of the *NPM1* mutational status, an AML genotype

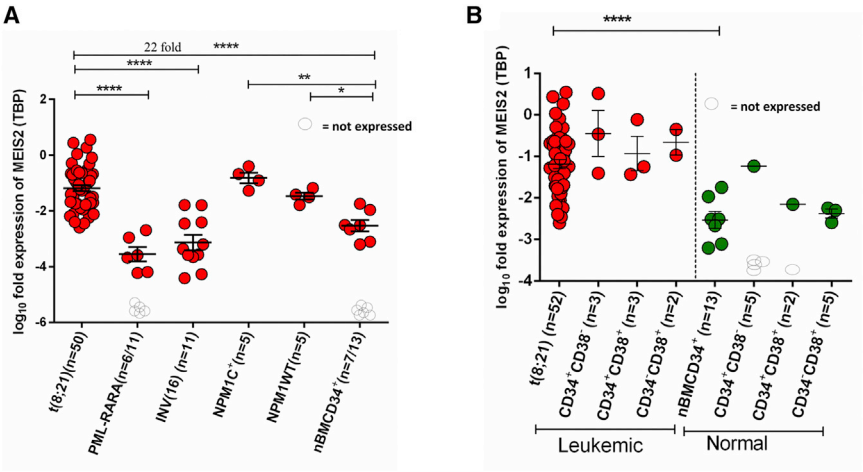

Figure 1. MEIS2 Expression in Patients with AML

(A) Quantification of *MEIS2* expression in core binding factor (CBF) and normal-karyotype AML. Expression levels of *MEIS2* in AML patients with *AE, PML-RARa* fusions, or Inv(16), and normal human BM $CD34^+$ cells were determined by qRT-PCR (relative to housekeeping gene TBP). *MEIS2* was expressed in 6/11 *PML-RARAa,* 11/11 *inv(16)*, and in 7/13 normal $CD34^+$ samples. All tested AE and $NPMc^+$ (n = 5) or NPM wild-type (WT) (n = 5) cases were positive for *MEIS2* expression. Expression values are shown as mean ± SEM. Statistical significance is indicated (****p < 0.0001).

(B) Quantification of *MEIS2* expression in leukemic and normal hematopoiesis. Expression levels of *MEIS2* of leukemic subpopulations of patients with *AE*-positive AML and normal BM subpopulations were determined by qRT-PCR (relative to housekeeping gene TBP). Bars show the mean ± SEM. *, not detectable (****p < 0.0001). *MEIS2* expression in normal $CD34^+/CD38^-$ (n = 1/5) and $CD34^+/CD38^+$ (n = 1/2); *, not detectable.

previously associated with elevated homeobox gene expression in contrast to *AE*-positive AML (n = 10). Importantly, the majority *AE*-positive AML cases showed significantly on average 22.3-fold-higher *MEIS2* transcript levels ($p < 0.005$) compared to normal human $CD34^+$ BM samples (Figure 1A). Furthermore, *MEIS2* was highly expressed in $CD34^+/CD38^-$ leukemic stem cell (LSC) candidates isolated from AE-positive cases (n = 3), whereas no expression of this gene was detectable in four of five samples of the corresponding normal counterpart (Figure 1B). Importantly, MEIS2 protein expression could be validated in representative t(8;21)-positive patients at levels comparable to normal human cord blood cells (Figure S1A).

In summary, these data indicate that *AE*-positive AML is characterized by aberrant expression of *MEIS2* in all leukemic compartments, including the most primitive $CD34^+/CD38^-$ compartment associated with LSC activity.

MEIS2 Collaborates with AE in Inducing AML

To test whether aberrant expression of *MEIS2* is of any functional relevance in human AML, the impact of small hairpin RNA (shRNA)-mediated *MEIS2* depletion in the AE-positive cell lines SKNO-1 or Kasumi-1 was analyzed. Knockdown of *MEIS2* by three independent shRNA constructs in vitro resulted in a significant reduction in proliferation and colony formation that was reflected in a statistically significant increase in the proportion of cells in G0/G1phase and also an increase in cells expressing the differentiation maker CD11b in SKNO-1 cells (Figures 2A–2C and S1B–S1E). The functional relevance of *MEIS2* expression was confirmed in a primary AE sample that showed 38% reduction in cell viability after small interfering RNA (siRNA)-mediated suppression of *MEIS2* expression in comparison to the scrambled control (Figure 2D).

To further validate collaboration of MEIS2 with AE, we tested expression of *Meis2* in normal murine hematopoiesis and mimicked co-expression of *Meis2* with the *AE* fusion gene in human AML by retrovirally engineered co-expression of MEIS2 and AE in murine progenitor cells. In line with our findings in normal human BM, *Meis2* expression was low in hematopoietic stem cells and absent in most samples of more differentiated hematopoietic cells (Figure S2A). AE collaborated significantly with MEIS2 as reflected in the colony forming unit-spleen (CFU-S) assay, increasing the median colony number on the spleen by 2.3-fold ($p < 0.05$) 12 days post-transplant compared to mice transplanted with cells carrying AE alone (Figure S2B). Mice transplanted with BM cells expressing constitutively AE, MEIS2, or GFP did not develop any disease up to 500 days post-transplantation. In contrast, mice injected with only 3.1% ± 2.3% transduced BM cells co-expressing both the AE fusion and MEIS2 developed AML 171 days after transplantation (n = 7), with an average engraftment of 92.4% ± 0.01% SEM and significant shortening of survival compared to the GFP control mice, indicating collaboration of both genes in vivo. Leukemias generated by AE and MEIS2 were transplantable and induced disease after a short latency of 33 days in secondary recipients (n = 11) (Figure 3A). Examination of the peripheral blood (PB) of diseased mice showed hyperleukocytosis, accumulations of blasts, splenomegaly, and severe multi-organ infiltration with leukemic blasts, which were highly positive for Mac1, Gr1, and c-Kit (Figures 3B, S2C, and S2D; Tables S2 and S3). According to the Bethesda criteria for hematological neoplasms, all mice in the AE/MEIS2 arm died of AML with maturation (Figure 3C).

In contrast to the observed synergy in leukemogenic activity between MEIS2 and AE, MEIS2 overexpression did not shorten disease latency when combined with the more potent *AML1-ETO9a (AE9a)* gene, previously shown on its own to be able to cause AML within 175 days (Yan et al., 2006) (Figures S2E–S2G). This was in line with results from the CFU-S assay, which did not show any differences in splenic colony formation between AE9a/MEIS2 and AE9a alone (Figure S2H). Of note, overexpression of AE9a was observed to enhance endogenous *Meis2* expression 6.2-fold (±1.60 SEM) in murine BM progenitor cells, a level of induction substantially higher than that seen with AE alone (3.05-fold [±0.48 SEM]) (Figure S2I). Importantly, there were no recurrent retroviral integration sites in both AE/MEIS2- and AE9a- or AE9a/MEIS2-positive leukemias enlisted

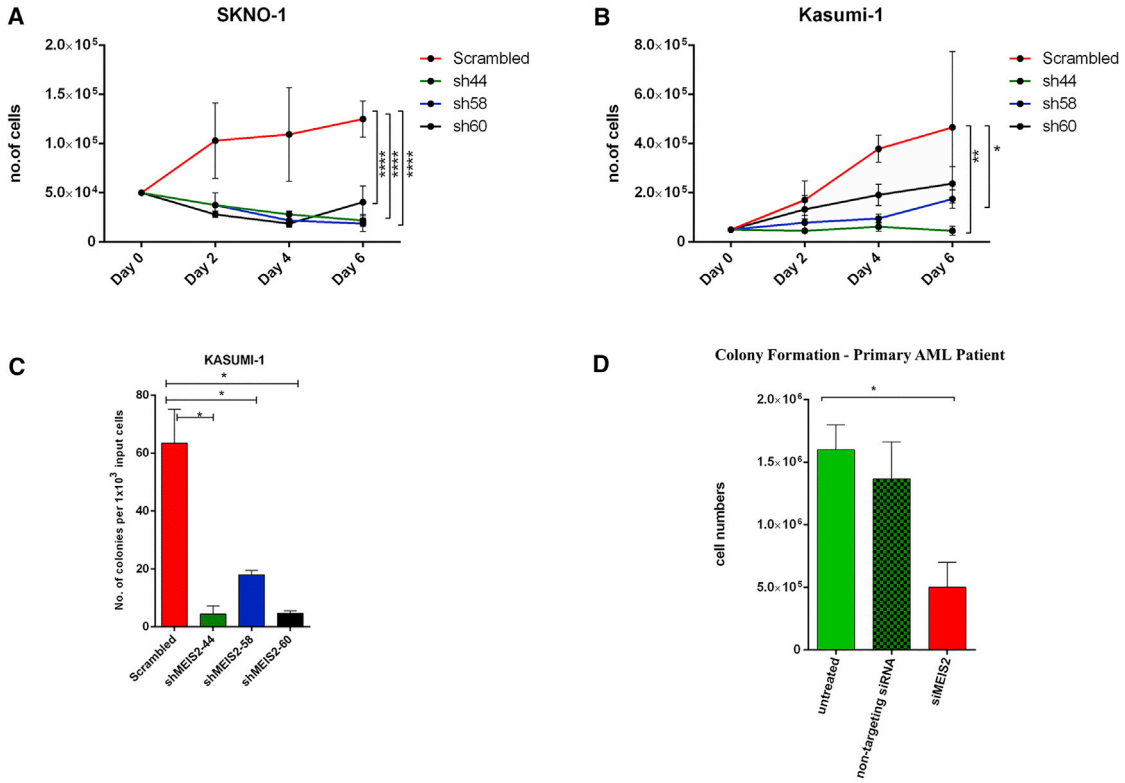

Figure 2. Impact of shRNA-Mediated Lentiviral Knockdown of *MEIS2* on t(8;21)-Positive AML Cell Lines and a t(8;21)-Positive Patient Sample

(A and B) Impact of knockdown (KD) of *MEIS2* compared to SCR control on (A) proliferation (n = 3 for SKNO-1 with KD of 31.85 ± 8.4 SEM for sh44, 43.8 ± 6.8 SEM for sh58, and 19.5 ± 2.78 SEM for sh60, respectively, and 42.7 ± 7.1 SEM for sh44, 30.5 ± 4.4 SEM, for sh58 and 30.9 ± 6.3 SEM for sh60, respectively) and (C) colony formation (n = 3 for Kasumi-1). Significance was calculated by two-way ANOVA (****p < 0.0001; ***p = 0.001; *p = 0.005).

(D) Impact of siRNA-mediated knockdown of *MEIS2* in a diagnostic, previously untreated patient sample having, as a sole cytogenetic abnormality, the translocation t(8;21) (no. 62 in Table S1) on cell number compared to SCR control (n = 1 in technical triplicates). Average knockdown efficiency was 54.2%; cell viability was measured 72 hr after siRNA induction.

in the retroviral tagged cancer genes database (RTCGD) (data not shown).

To characterize genes and pathways differentially expressed by overexpression of MEIS2 and *AE*-positive cells, we performed microarray analyses 48 hr after successful gene transduction in 5-fluorouracil (5-FU)-mobilized murine progenitor cells. In comparison to the GFP control, MEIS2 with AE induced upregulation of 75 probesets corresponding to 23 genes and downregulation of 159 probesets corresponding to 122 genes. In contrast to the upregulated genes, the vast majority of downregulated genes did not overlap between AE/MEIS2 and AE alone (Figures S3A and S3B; Table S4). When these differentially expressed genes between AE/MEIS2 and GFP were analyzed in the Kyoto Encyclopedia of Genes and Genomes (KEGG)-based pathway analysis, "cytokine-cytokine receptor interaction," "transcriptional misregulation in cancer," and "pathways in cancer" scored among the top-five ranking categories. In a direct comparison between AE and AE/MEIS2 BM, out of 195 differentially regulated probesets referring to 145 genes, 29 probesets (12 genes) were upregulated and 166 probesets (80 genes) were downregulated (Table S4). Interestingly, *Hoxa* genes such as *Hoxa5*, *Hoxa7*, *Hoxa9*, and *Hoxa10* were downregulated in *AE* and *AE/MEIS2* compared to the empty vector. This was further validated by qRT-PCR, indicating that the leukemogenicity of AE/MEIS2 does not depend on upregulation of oncogenic *Hoxa* genes (Figures S3C and S3D). Gene set enrichment analysis (GSEA) analysis for oncogenic signature (MsigDB version 5.0) showed enrichment for gene sets such as "*JAK2*" and "*PTEN*" in AE/MEIS2 versus AE alone (Figure S3E; Table S4). Consistent with the finding that MEIS2 did not increase leukemogenicity of AE9a, RNA-seq of leukemic BM showed a close overlap in gene expression between AE9a and AE9a/MEIS2, indicating that adding of MEIS2 to the leukemogenic truncated AE9a does not induce gross changes in the molecular phenotype of *AE9a*-positive leukemias (Figures S3F and S3G).

Taken together, these data indicate that MEIS2 functionally collaborates with AE in AML.

MEIS2 Binds to AE

To understand the mechanism of AE-MEIS2 collaboration, we first sought to identify domains of the fusion gene that may be critical for collaboration between AE and MEIS2 using the CFU-S assay as readout for growth-promoting activity (Figures S4A and S4B). Only the inactivating point mutation in the Runt

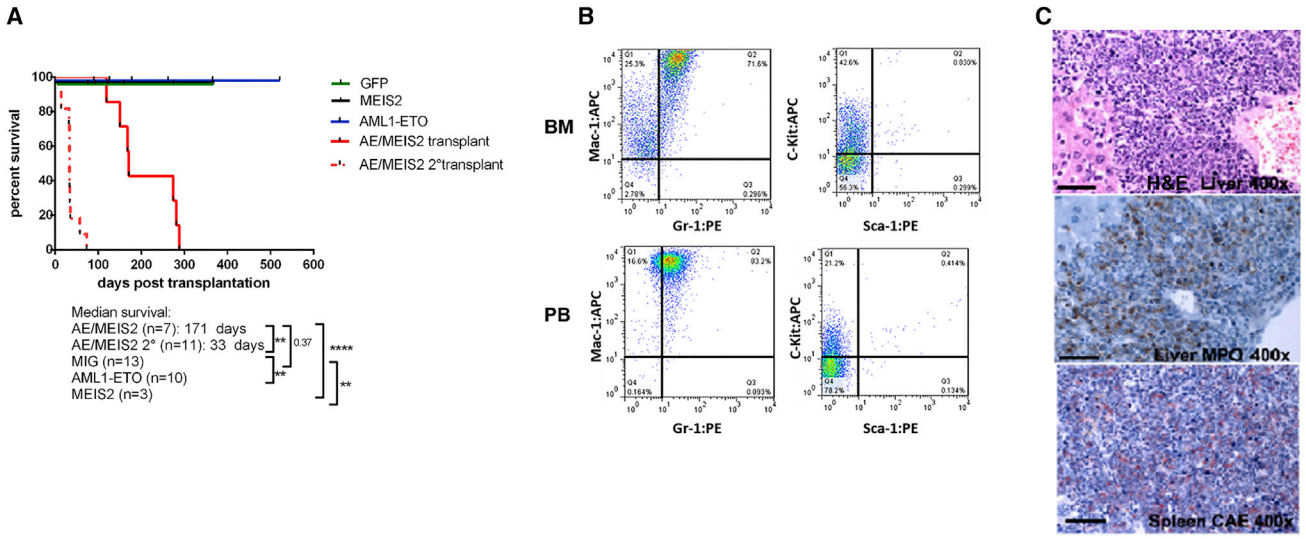

Figure 3. Co-expression of MEIS2 and AML1-ETO Induces AML in Mice

(A) Survival plot of mice transplanted with AE and MEIS2. Kaplan-Meier survival curves of mice transplanted with BM cells expressing AML1-ETO (AE), MEIS2, the empty GFP control vector, or AE/MEIS2. Survival of secondary recipients transplanted with BM of diseased primary AE/MEIS2 mice is shown in addition. Log-rank Mantle-Cox test was used to calculate the statistical significance as indicated (**p < 0.005; ****p < 0.0001; ***p = 0.0001; **p = 0.001).

(B and C) Dot plot of a representative leukemic *AE/MEIS2* mouse (B) and histological analysis of different organs (C). Immunophenotyping and histology of BM and PB of a representative mouse diagnosed with AML is given (mouse no. 10; Table S3). Samples were gated for GFP-positive cells. MPO, myeloperoxidase; CAE, N-acetyl-chloroacetate esterase. Histology pictures are magnified 400×. Scale bar, 50 μm.

domain, not deletion of the NHR1 or C-terminal stretch, reduced collaboration between MEIS2 and the fusion gene, indicating that DNA binding properties are crucial for AE-MEIS2 leukemogenic collaboration. There was a trend that MEIS2 could further enhance CFU-S activity of the C-terminally truncated Δ540 AE construct that contains the TAF/NHR1 domain and lacks the zinc-finger domains, previously shown to have similar activity as the wild-type *AE* (Westendorf et al., 1998) (Figure S4C). To test for a possible direct interaction between AE and MEIS2, co-immunoprecipitation (coIP) assays along with various other mutants of MEIS2 (Figure S4D) were performed in HEK293 cells. Surprisingly, strong binding of MEIS2 to the Runt domain of AE could be documented (Figures 4A and 4B). Additional experiments showed that AE9a is also able to strongly bind to MEIS2 (Figure S4E) and that the N-terminal region (amino acids [aa] Δ1–68 or 69–470) of MEIS2 is critical for binding to the Runt domain of AE and AE9a (Figures 4C, 4D, S4E, and S4F). The binding of MEIS2 to AE was validated in a human leukemic background by performing immunoprecipitation for ETO and western blotting for MEIS2 in the AE-positive human cell line SKNO-1 (Figure S4G). To test whether hematopoietic activity of MEIS2 depends on binding to AE, we generated a mutant with deletion of 1–68 aa N-terminally (MEIS2(69–470)), which has lost its binding capacity to the fusion gene (Figure 4D). In contrast to the wild-type MEIS2, which induced significantly more colonies in collaboration with AE than AE alone, MEIS2(69–470) plus AE failed to increase colony numbers compared to AE alone. This could be re-confirmed in secondary re-plating assays, which also showed a significant loss of activity of the AE/MEIS2 (69–470) combination compared to AE/MEIS2. Similarly, at the level of CFU-S, AE/MEIS2 increased spleen colony numbers significantly compared to AE alone in contrast to the AE/MEIS2 (69–470) combination. This was further confirmed in the more sensitive ΔCFU-S assay, which showed a lack of collaboration between AE and MEIS2 (69–470) (Figures S4H–S4J). Collectively, these data provide evidence that MEIS2 is able to directly interact with the most frequent fusion gene in AML and that binding to AE is critical for its full collaborative activity in the CFU-S assay.

MEIS2 Alters Target Gene Binding of AE

To analyze whether MEIS2 expression levels impact AE DNA binding properties, chromatin immunoprecipitation (ChIP) sequencing was performed in the human AE-positive Kasumi cell line after shRNA-mediated MEIS2 knockdown (shMEIS2-44) compared to the scrambled control, using an AE fusion-specific antibody (Martens et al., 2012). Successful enrichment for AE target genes by the antibody used was first validated by ChIP qPCR for known specific binding partners of AE such as *SPI1*, *OGG1*, *FUT7*, and *NFE2,* each of which showed substantial enrichment (showing an up to 18-fold) (Figures S5A and S5B). In addition, motif analyses of the AE binding sites in the ChIP-seq revealed enrichment for both the *RUNX1* and *ETS1* target sites as previously reported (Martens et al., 2012) in both experimental arms, comprising between 35% and 42% of all target regions, as well as the presence of weaker motifs with 44.32% and 65.8% for scrambled (SCR) and shMEIS2, respectively (Figures S5C–S5F; Table S5). As we observed increased binding of AE to RUNX1 after MEIS2 knockdown, changes in expression of *RUNX1* were tested in the t(8;21)-positive cell lines SKNO-1 and Kasumi after *MEIS2* depletion: however, knockdown induced no major change of *RUNX1* expression in both cell lines (n = 3) (data not shown).

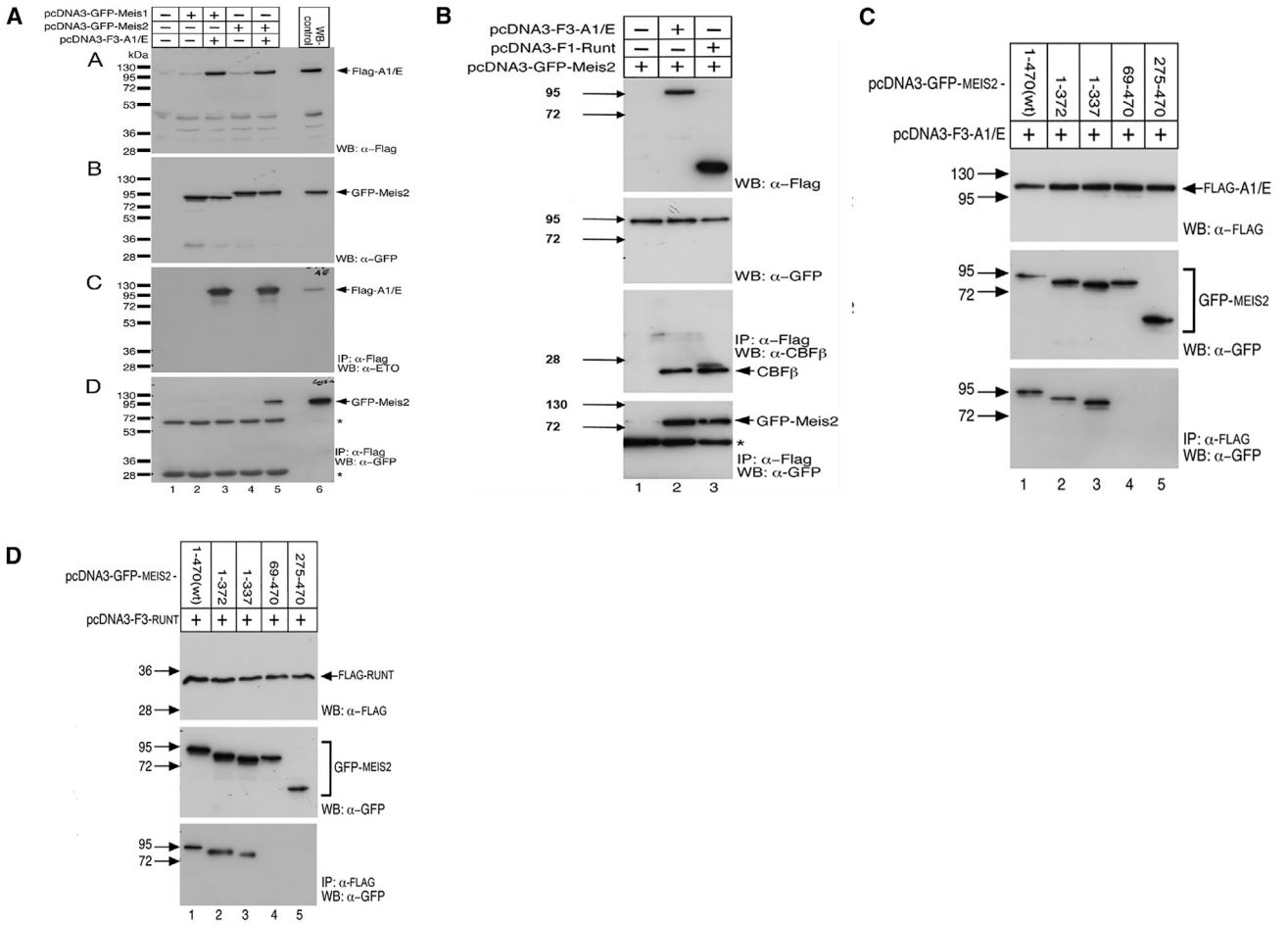

Figure 4. Co-immunoprecipitation Assays on AE and MEIS2 Interaction in HEK293 Cells

(A) Immunoprecipitation (IP) of FLAG-AE and western blot using anti-FLAG and anti-ETO (for AE) and anti-GFP (for MEIS2) antibodies, respectively. Interaction of MEIS2 with AE is shown in lane 5.

(B) IP of FLAG-RUNT and FLAG-AE and western blot using anti-FLAG (for RUNT and AE) and anti-GFP (for MEIS2), antibodies, respectively. MEIS2 interacts with AE and to the RUNT domain of AE (lane 3). *Immunoglobulin G (IgG) heavy chains (in C heavy and light IgG chains).

(C and D) Additional mutants of MEIS2 were generated to map the interacting domain of full-length AE and RUNT with MEIS2. WT MEIS2 and all the mutants interacted strongly with AE and RUNT, except the N-terminally deleted mutants Δ1–68 (aa 49–470) and Δ1–274 (aa 275–470).

At a cutoff of ≥10-fold with a FDR rate threshold of 0.001 and a FDR effective Poisson threshold of 0, a total of 13,003 high-confidence DNA binding regions for AE with or without expression of shMEIS2 were detectable. Of note, knockdown of *MEIS2* increased the number of AE binding sites compared to the control by >2-fold. In addition, knockdown of the *MEIS2* gene induced >7,900 unique AE binding sites, indicating gross changes in the DNA binding behavior of the fusion gene after MEIS2 depletion (Figure 5A). When we focused on the promoter regions (defined as binding regions 1 kb upstream and 100 bp downstream of the transcription start site), AE still bound to significantly more DNA sites after *MEIS2* knockdown, with >1,100 unique binding sites compared to the control (Figure 5B; Table S4). The higher number of AE DNA binding sites after MEIS2 depletion was a consistent characteristic throughout the differentially annotated DNA regions (Figure 5C). Among those genes that showed substantial increase of AE binding after MEIS2 knockdown were *IGFBP7*, *mir-4442*, *OGG1*, *RUNX1*, and *WT1*. A smaller proportion of genes showed decreased AE binding after MEIS2 depletion, such as *mir-145*, *NDUFA4*, and *KRAS* (Figure S6A). Other genes did not meet the above-mentioned criteria for AE binding in the scrambled control but met the requirements with a >10-fold increase in AE binding, such as ASLX2, FLT3, CREB1, GSK3a, and HMGA1 (Table S6). Of note, expression of MEIS2 decreased after AE shRNA-mediated knockdown in SKNO-1 cells, although there was no documented binding of AE to the MEIS2 promoter (Figures S6B and S6C).

Thus, these data demonstrated that high MEIS2 expression is associated with a reduction of AE binding to DNA targets and, vice versa, that knockdown of MEIS2 increases AE binding sites. Furthermore, the data show that AE binds to a distinct and unique set of DNA sites in human AML cells when MEIS2 is highly expressed.

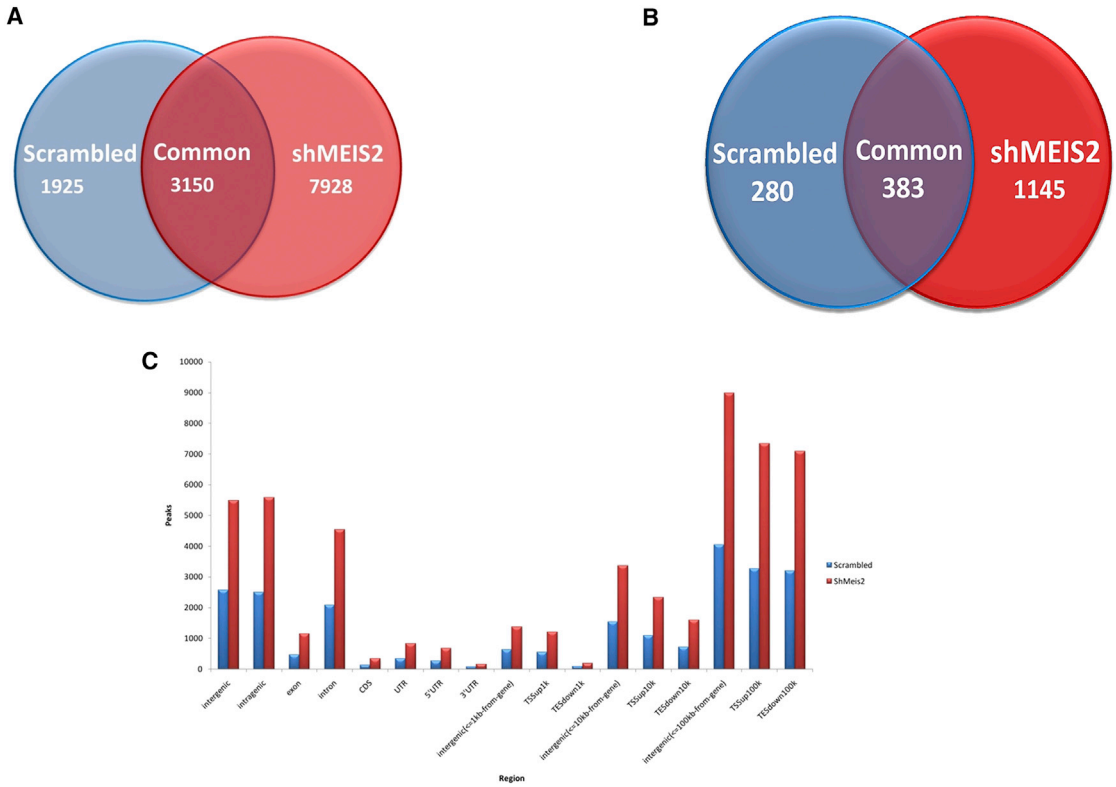

Figure 5. AE Binding Sites

(A) Venn diagram showing the number and overlap of all genomic AE binding sites in Kasumi-1 cells after knockdown of MEIS2 (shMEIS2-44) compared to the SCR control.

(B) Venn diagram showing the number and overlap of genomic AE binding sites in the promoter region (the annotated peaks that are 1 kb upstream of the TSS and 100 bp downstreak of the TSS) in Kasumi-1 cells after knockdown of MEIS2 (shMEIS2-44) compared to the SCR control.

(C) Distribution of the AE binding sites in the genome (relative to RefSeq genes). TSS, transcriptional start site; TES, transcriptional end site.

High Expression of MEIS2 Is Associated with Loss of AE Binding to the YES1 Promoter Region and Increased YES1 Expression

To correlate AE target gene binding with expression levels, RNA-seq was performed in parallel to ChIP sequencing (ChIP-seq) for the same samples in duplicates. Genes were considered as differentially expressed when the difference in FPKM (fragments per kilobase per millions reads) was significant at a p value of 0.05, with a false discovery rate (FDR) of 0.05. First, differentially expressed genes were analyzed independent of AE target binding: 868 genes were differentially expressed between Kasumi cells transduced with the *MEIS2* shRNA versus scrambled control (Table S4). KEGG analysis showed changes in the expression of genes belonging to the categories ribosomes, lysosomes, and adherence junction (Tables S4 and S7). Of note, *MEIS2* knockdown induced major differences in gene expression, with an up to 2.25 log2 fold change for upregulated genes (n = 365) and up to 9 log2 fold for downregulated genes (n = 123 genes) compared to the SCR control (Table S4).

As a second step, we correlated differentially expressed genes with AE DNA binding. Among the genes with changes in expression and AE binding, there were two categories. The first showed an increase in expression accompanied by an enhanced AE binding to their promoter region (e.g., *MPO*, *KIT*, *NUCB2*, and *CD34 MYOG1*). The second group showed decreased expression level parallel to increased AE binding (e.g., *YES1*, *BCL2L1*, *HMGA1*, *IGFBP2*, and *TXNIP*) after *MEIS2* knockdown (Table S8). We validated these findings for selected genes and found a significant ($p < 0.05$) positive correlation between expression levels determined by RNA-seq and qRT-PCR (Figure S6D). There was no decrease in the expression of the targetable receptor tyrosine kinases c-Kit and *FLT3* after *MEIS2* knockdown as validated by qRT-PCR. In contrast, knockdown of *MEIS2* induced a substantial decrease in expression of the Src kinase *YES1* accompanied by increased AE promoter binding of this gene (Figure 6A). This finding thus provided an intriguing gene whose expression was strongly dependent on MEIS2 overexpression and whose effects were potentially druggable. Of note, knockdown of *YES1* resulted in an up to 78% reduction in proliferation and 95% reduction in clonogenic growth in Kasumi cells (Figures 6B–6D), indicating that *YES1* expression is relevant for the cell growth of this AE-positive AML cell line. This was in line with the observation that knockdown of *Yes1* in primary leukemic murine AE9a/MEIS2 cells impaired primary clonogenic growth by, on average, 70.5% (sh84) and 71.14% (sh152) and re-plating by 93.98% and 69.13% for the two

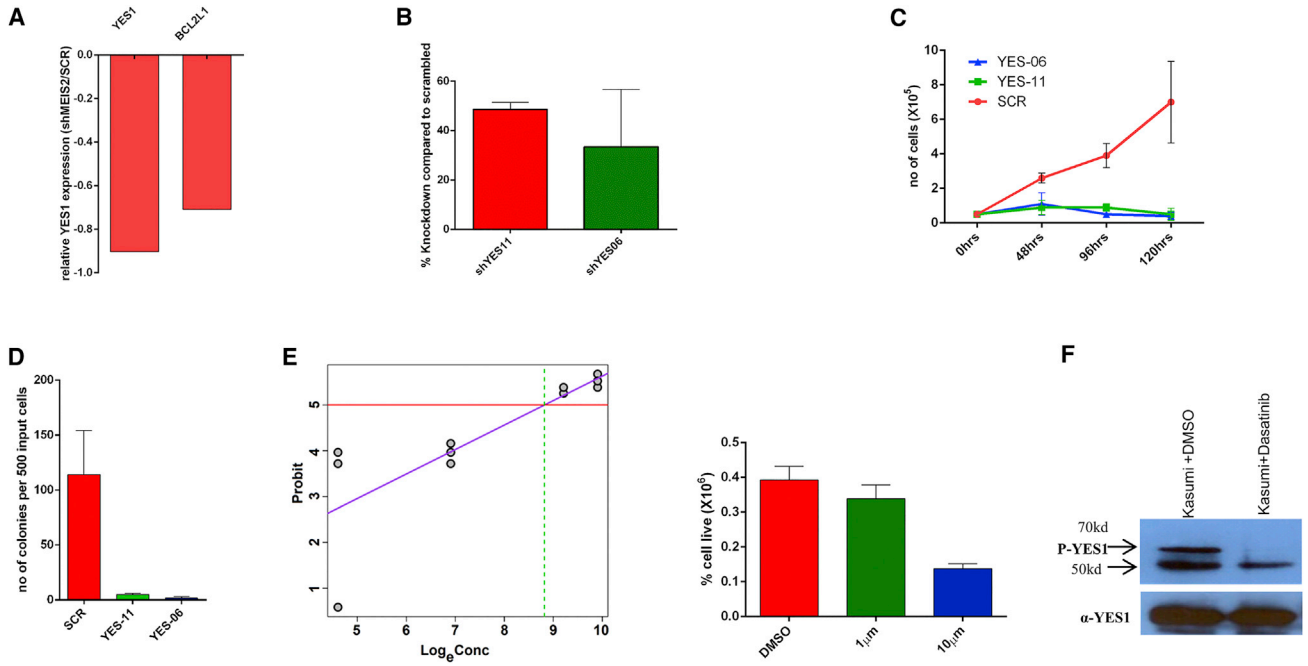

Figure 6. *YES1* Expression after *MEIS2* Knockdown

(A) Expression of *YES1* after *MEIS2* knockdown in Kasumi cells determined by qRT-PCR and RNA-seq showing downregulation of the kinase.

(B) Percentage of YES1 knockdown in Kasumi cells.

(C) Cell growth of Kasumi cells after YES1 knockdown compared to SCR control (n = 3).

(D) Colony formation after YES1 knockdown compared to SCR control (n = 3; mean ± SEM).

(E) 2 × 10^5 Kasumi-1 cells were treated with dasatinib at different concentrations for 72 hr, resulting in an IC_{50} value of 6.8 μm (calculated on the basis of live cells with probit = 5 [50% effect]; Y = 0.53 $\log_e$ concentration + 0.28 sigmoid model). Bar graphs (mean ± SEM) show that dasatinib concentrations between 1,000 nm and 10,000 nm resulted in >50% cell growth inhibition after 72 hr.

(F) IP of YES1 and western blotting for p-YES1 in Kasumi-1 cells treated with DMSO or 6.8 μm dasatinib for 72 hr, demonstrating loss of phosphorylation after dasatinib treatment.

shRNAs, respectively (Figures S6F–S6H). Indeed, all AML genotypes, including the AE-positive AML subtype showed YES1 expression as previously indicated in The Cancer Genome Atlas (TCGA) database (Network, 2013) (Figure S6E). Next, we tested the efficacy of pharmacological YES1 inhibition. So far, there are no selective YES1 inhibitors available. One of the most potent YES1 inhibitors is dasatinib, which also impairs other kinases such as c-Src, Fyn, and Lyn (BMS-354825) (Patel et al., 2013). The AE-positive Kasumi cell line, expressing high levels of *MEIS2*, is also positive for YES1 expression and showed complete loss of phosphorylation of the kinase after dasatinib treatment. With a half maximal inhibitory concentration (IC_{50}) value of 6.8 μM, dasatinib was highly efficient in impairing Kasumi cell growth in vitro (Figures 6E and 6F). Although it has to be taken into account that dasatinib is a multikinase inhibitor known to target several other kinases such as Lyn, PDGFR, KIT, Lck, Fyn, and c-Src, these data at least suggest that YES1 is an attractive target in AE-positive AML.

All together, these data point to a regulatory network, in which high MEIS2 expression collaborates with AE in inducing leukemia, involving at least in part MEIS2's ability to strongly bind to AE and thereby grossly change binding of AE to its target genes on a global scale. This results in loss of repression of proto-oncogenes, exemplified by an increase in the expression of the YES1 kinase in AML cells, thereby opening avenues to link a leukemogenic liaison between transcription factors to a druggable target.

DISCUSSION

AML characterized by the translocation t(8;21) counts for 15% of all human AML cases and is characterized by expression of the most frequent fusion gene detectable in patients with this disease. So far, the AE-positive AML genotype was not associated with deregulated homeobox gene expression (Andreeff et al., 2008; Lo et al., 2012). In this report, we now provide evidence that TALE homeobox genes are involved in AE leukemogenesis and that they can directly interact with the fusion gene. We initiated the study quantifying the expression of the TALE homeobox gene *MEIS2* in a larger AML patient cohort and could readily demonstrate that *MEIS2* is aberrantly highly expressed not only in virtually all AE-positive AML cases compared to normal $CD34^+$ hematopoiesis but also in comparison to other core binding factor (CBF) leukemias. The mechanism behind this observation is unclear. Despite the gross differences in *MEIS2* expression between AE AML samples and normal $CD34^+$ BM cells, both populations did not show any major methylation differences at the CpG regions of the *MEIS2* promoter as determined by MassARRAY technology, indicating that expression of this gene is not regulated by

methylation, at least of these CpG islands (data not shown). Interestingly, published microarray data documented a significantly and 4.3-fold (log_2) increased expression of *MEIS2* after retrovirally induced overexpression of AE in human $CD34^+$ cord blood cells compared to the control (expression atlas EMBL-EBI; Krejci et al., 2008), in line with our own data showing the same observation for murine progenitor cells, whereas in the human setting, a reduction of MEIS2 expression after knockdown of AE was only observed in the t(8;21)-positive SKNO-1 cell line and not in Kasumi cells (data not shown). The mechanism of this is not clear, as we did not see any major binding of AE to the *MEIS2* region, as also described by Ptasinska et al. (Ptasinska et al., 2012).

Functional relevance of high *MEIS2* expression in collaboration with AE could be clearly demonstrated by knockdown in human AML cells and in the BM transplantation assay, in which only MEIS2, in collaboration with AE, induced leukemia in contrast to MEIS2 or AE alone, as shown by us and several other groups (de Guzman et al., 2002; Fenske et al., 2004; Licht, 2001; Schessl et al., 2005). However, in our model, the latency time until development to AML was long, with a median time of 171 days until disease post-transplant. The long latency suggests that MEIS2 in concert with the human full-length AE fusion gene needs additional partners. To test how this homeobox gene might functionally interconnect with AE, we analyzed binding between the two proteins and surprisingly found strong binding between MEIS2 and AE. Interaction between endogenous MEIS2 and AE could be re-confirmed in the human AML SKNO-1 cell line. These results thus implicate a previously unrecognized direct interaction between AE and MEIS2 in human AML. An important question is whether direct binding to AE is relevant for the collaboration between MEIS2 and AE. To address this, we generated a mutant that lost binding to AE. Importantly, this construct showed reduced hematopoietic activity compared to the full-length protein. *MEIS2* was also highly expressed in AML cases with NPM1 mutation or normal karyotype with an NPM1 wild-type protein, and shRNA-mediated knockdown of MEIS2 impaired growth in a panel of AML cell lines harboring, among others, NPM1 mutation or a MLL fusion (data not shown). This might indicate that high MEIS2 expression contributes to leukemogenesis in other AML genotypes. It will be important in future work to analyze this in more detail and to understand possible AE-independent mechanisms of MEIS2 leukemogenicity. We also tested binding of MEIS2 to the truncated AE9a oncogene and proved that MEIS2 is also able to bind strongly to this AE isoform. However, we did not see acceleration of AE9a induced disease by MEIS2 co-expression, in line with published data demonstrating rapid onset of leukemia by AE9a alone in contrast to the full-length AE fusion (Yan et al., 2006). Complex formation between TALE homeobox genes such as *Meis1* and *Pbx1* has been described and is essential for mediating *Hoxa9* leukemogenicity (Kroon et al., 1998; Shen et al., 1999), but so far, there are no reports on complex formation between TALE homeobox genes and the AE fusion gene. With regard to AE, the fusion gene might have a completely different DNA occupancy when interacting with MEIS proteins. Indeed, we could demonstrate that AE changes its DNA binding properties significantly after shRNA-mediated MEIS2 knockdown in human AML cells. According to the ChIP-seq data presented in this work, AE DNA binding occupancy in AML cells was substantially reduced when MEIS2 was highly expressed. Conversely, *MEIS2* knockdown resulted in a gross and >100% increase in the number of AE binding sites, accompanied by a significant impairment of AML cell growth. This suggests that MEIS2 might promote AE-associated leukemogenesis by impairing or restricting binding of a repressive AE complex to proto-oncogenes, resulting in a critical increase of potentially oncogenic AE targets (Ptasinska et al., 2012). This increase in AE binding was observed for several known genes involved in cell activation, growth, and cancer such as *KIT*, *MPO*, *HMGA1*, *CD34*, and *IGFBP7* (Ptasinska et al., 2012) or *YES1* and *MAPK1* (Maiques-Diaz et al., 2012). However, changes in AE binding to *KIT* did not result in changed expression in contrast to YES1. This SCRSrc kinase has previously been described as one of the key members of a gene set of AE targets with an AML1 binding site, co-occupied by the histone deacetylase 1 and characterized by a dramatic loss of H4 hyperacetylation marks. Interestingly, this study classified YES1 among the target genes of AE (Maiques-Diaz et al., 2012). We could also demonstrate that high expression of MEIS2 can impair AE binding to the YES1 promoter, resulting in an increased expression of this proto-oncogene in human AML cells. Additionally, knockdown of YES1 abrogated the growth of AE-positive AML as well as primary leukemic BM. Unfortunately, to date, no selective YES1 kinase inhibitor is available. Among the most potent YES1 inhibitors is dasatinib, which also blocks other src kinases (Patel et al., 2013). Although the data have to be interpreted with caution based on this, dasatinib a highly potent blocker of growth of AE-positive cells, and this was accompanied by dephosphorylation of the YES1 protein. Interestingly, clinical trials are ongoing in AE-positive AML to test the efficacy of dasatinib as an addition to chemotherapy or as a single agent (Boissel et al., 2015; Marcucci et al., 2013). All of this illustrates that the leukemogenic collaboration of MEIS2 and AE can be mechanistically linked to kinases, which opens an avenue for targeting this leukemogenic liaison between the two transcription factors by approved drugs such as dasatinib.

Altogether, these data shed light on an unexpected leukemogenic crosstalk between the most frequent fusion gene in AML and the MEIS2 homeobox gene, identifying MEIS2 as a potent collaborative leukemogenic partner that affect DNA binding of the most frequent fusion gene in human AML.

EXPERIMENTAL PROCEDURES

Patient Samples, Cell Lines, and Mouse Experiments

Mononuclear cells isolated from diagnostic BM or PB with AML leukemias from 92 adult patients were analyzed (n = 70 for *t(8;21)*, n = 11 for *PML-RARa*, n = 11 for *inv (16)*, and n = 5 for *NPM-WT and NPMC*$^+$). $CD34^+$ from bone marrow mononuclear cells (BM MNCs; Lonza) (n = 13) from healthy individuals were taken as controls. Cytochemistry and cytogenetics (Table S1) were performed in all cases as described. Cases were classified according to the French-American-British criteria and World Health Organization classification (Bennett et al., 1976; Harris et al., 1999). The study was approved by the ethics committees of all participating institutions, and informed consent was obtained from all patients before they entered the study in accordance with the Declaration of Helsinki (http://www.wma.net/en/30publications/10policies/b3/index.html). The *t(8;21)*-positive AML cell lines Kasumi-1 (all DMSZ) and SKNO-1 (kindly provided by Michael Lübbert, Freiburg, Germany) were used for expression analysis. Kasumi-1 and OCI-AML3 were cultured in RPMI 1640 with 20% fetal bovine serum (FBS) and

1% penicillin-streptomycin. SKNO-1 was cultured in RPMI 1640 medium with 10% FBS + granulocyte-macrophage colony-stimulating factor (GM-CSF) (10 ng/ml). Mice experiments were performed in compliance with the German Law for Welfare of Laboratory Animals and were approved by the Regierungspräsidium Tübingen, Germany.

Co-immunoprecipitation and Western Blotting

Cell lines HEK293 (ATCC, CRL 1573) and HeLa (ATCC, CCL 2) were grown in DMEM (Gibco) supplemented with 10% fetal calf serum (FCS), penicillin, and streptomycin. HEK293 and HeLa cells were transfected using the Nanofectin transfection reagent (PAA) according to the manufacturer's instructions. For western blotting and immunoprecipitation (IP) experiments whole-cell lysates were prepared as described previously (Salat et al., 2008; Wacker et al., 2011). Protein concentrations were determined using the Bradford assay method (Bio-Rad). Details regarding coIP and western blot can be found in Supplemental Experimental Procedures.

ChIP-Seq and Peak Detection

Chromatin was harvested as described previously (Denissov et al., 2007). ChIP was performed using specific antibodies to AE (Diagenode, C15310197) and analyzed by qPCR or ChIP-seq as previously described (Martens et al., 2012). Primers for qPCR used were as follows:

SPI1: forward, 5′-GGGTAAGAGCCTGTGTCAGC-3′; reverse, 5′-CAGATGCACGTCCTCGATAC-3′
FUT7: forward, 5′-TGAAACCAACCCTCAAGGTC-3′; reverse, 5′-TCACTGGCATGAATGAGAGC-3′
NFE2: forward, 5′-GGTTAGCAGCATACGTGGAG-3′; reverse, 5′-ACGATACGGAGAAAACCACG-3′
OGG1: forward, 5′-CCACCCTGATTTCTCATTGG-3′; reverse, 5′-CAACCACCGCTCATTTCAC-3′
VAV1: forward, 5′-AGAAGGGTTTGAGGGCTAGG-3′; reverse, 5′-CTGTTACCAGGGCTTGGTTG-3′
H2B: forward, 5′-TGCATAAGCGATTCTATATAAAAGCG-3′; reverse, 5′-ATAAAGCGCCAACGAAAAGG-3′
MYOG: forward, 5′-AAGTTTGACAAGTTCAAGCACCTG-3′; reverse, 5′-TGGCACCATGCTTCTTTAAGTC-3′.

Relative occupancy was calculated as fold over background, for which the second exon of the myoglobin gene or the promoter of the *H2B* gene was used.

Illumina sequencing was done as previously described (Martens et al., 2010). Briefly, end repair was performed using the precipitated DNA of ~30 million cells using Klenow and T4 PNK. A 3′ protruding A base was generated using Taq polymerase, and adapters were ligated. The DNA was loaded on gel and a band corresponding to ~300 bp (ChIP fragment + adapters) was excised. The DNA was isolated, amplified by PCR, and used for cluster generation on the Illumina genome analyzer. Fastq files were quality controlled and adaptor trimmed using trimm galore (Martin, 2011), and sequences with phred score of 20 or higher were considered for downstream analysis. Sequences were then aligned to the human genome version hg19 using bowtie2 (Barbie et al., 2009). Peak calling and annotation was done using CisGenome (Ji et al., 2008) and HOMER v3.12 (http://homer.salk.edu/homer/ngs/peaks.html).

RNA-Seq and Analysis

RNA-seq was performed using libraries prepared by TruSeq RNA Sample preparation Kit version 2. The samples were run on HiSeq2000. After trimming Illumina sequencing adapters using trimm galore (Martin, 2011), high-quality raw Fastq files (phred score of 20 or higher) were aligned using tophat and respective RefSeq files (the human Hg19 assembly and the murine mm10 genome version). Differential expression analysis was performed using Cufflinks (Trapnell et al., 2009, 2010) and R packages (Team, 2013).

ACCESSION NUMBERS

The accession numbers for the microarray, ChIP-seq, and RNA-seq (Kasumi cell and murine leukemic BM samples) are GEO: GSE81174, GSE81321, GSE81328, and GSE81329, respectively.

SUPPLEMENTAL INFORMATION

Supplemental Information includes Supplemental Experimental Procedures, five figures, and eight tables and can be found with this article online at http://dx.doi.org/10.1016/j.celrep.2016.05.094.

AUTHOR CONTRIBUTIONS

N.M.V., J.K., F.O., V.N.T., A.M., J.H.A.M., V.P.S.R., L.Q.-M., K.F., S.B., and T.M. performed research and analyzed the data. J.H.A.M. and M.A.W. performed the sequencing analysis. K.S., W.H., K.D., H.D., and H.G.S. contributed research material. N.M.V., J.K., M.A.W., V.P.S.R., M.F.-B., and C.B. contributed to data interpretation. N.M.V. and C.B. wrote the manuscript, and C.B. designed the project.

ACKNOWLEDGMENTS

The authors would like to thank all members of the Core Facility FACS, Core Facility Genomics of the University Ulm and the animal facility of the Helmholtz Centre Munich and the University Ulm for breeding and maintenance of the animals. We want to thank R.K. Humphries for editing the manuscript. The work was supported by grants from the Bundesministerium für Bildung und Forschung (NGFN2 grant 01GS0448), the DFG (SFB 1074 project Z1, project A3 to FO and A6 to M.F.-B. and V.P.S.R.), and the Helmholtz Alliance Preclinical Comprehensive Cancer Center (to C.B.).

Received: December 4, 2014
Revised: April 20, 2016
Accepted: May 27, 2016
Published: June 23, 2016

REFERENCES

Alharbi, R.A., Pettengell, R., Pandha, H.S., and Morgan, R. (2013). The role of HOX genes in normal hematopoiesis and acute leukemia. Leukemia *27*, 1000–1008.

Andreeff, M., Ruvolo, V., Gadgil, S., Zeng, C., Coombes, K., Chen, W., Kornblau, S., Barón, A.E., and Drabkin, H.A. (2008). HOX expression patterns identify a common signature for favorable AML. Leukemia *22*, 2041–2047.

Argiropoulos, B., Yung, E., and Humphries, R.K. (2007). Unraveling the crucial roles of Meis1 in leukemogenesis and normal hematopoiesis. Genes Dev. *21*, 2845–2849.

Barbie, D.A., Tamayo, P., Boehm, J.S., Kim, S.Y., Moody, S.E., Dunn, I.F., Schinzel, A.C., Sandy, P., Meylan, E., Scholl, C., et al. (2009). Systematic RNA interference reveals that oncogenic KRAS-driven cancers require TBK1. Nature *462*, 108–112.

Bennett, J.M., Catovsky, D., Daniel, M.T., Flandrin, G., Galton, D.A., Gralnick, H.R., and Sultan, C. (1976). Proposals for the classification of the acute leukaemias. French-American-British (FAB) co-operative group. Br. J. Haematol. *33*, 451–458.

Boissel, N., Renneville, A., Leguay, T., Lefebvre, P.C., Recher, C., Lecerf, T., Delabesse, E., Berthon, C., Blanchet, O., Prebet, T., et al. (2015). Dasatinib in high-risk core binding factor acute myeloid leukemia in first complete remission: a French Acute Myeloid Leukemia Intergroup trial. Haematologica *100*, 780–785.

Bürglin, T.R. (1997). Analysis of TALE superclass homeobox genes (MEIS, PBC, KNOX, Iroquois, TGIF) reveals a novel domain conserved between plants and animals. Nucleic Acids Res. *25*, 4173–4180.

de Guzman, C.G., Warren, A.J., Zhang, Z., Gartland, L., Erickson, P., Drabkin, H., Hiebert, S.W., and Klug, C.A. (2002). Hematopoietic stem cell expansion and distinct myeloid developmental abnormalities in a murine model of the AML1-ETO translocation. Mol. Cell. Biol. *22*, 5506–5517.

Denissov, S., van Driel, M., Voit, R., Hekkelman, M., Hulsen, T., Hernandez, N., Grummt, I., Wehrens, R., and Stunnenberg, H. (2007). Identification of novel functional TBP-binding sites and general factor repertoires. EMBO J. *26*, 944–954.

Faber, K., Bullinger, L., Ragu, C., Garding, A., Mertens, D., Miller, C., Martin, D., Walcher, D., Döhner, K., Döhner, H., et al. (2013). CDX2-driven leukemogenesis involves KLF4 repression and deregulated PPARγ signaling. J. Clin. Invest. *123*, 299–314.

Fenske, T.S., Pengue, G., Mathews, V., Hanson, P.T., Hamm, S.E., Riaz, N., and Graubert, T.A. (2004). Stem cell expression of the AML1/ETO fusion protein induces a myeloproliferative disorder in mice. Proc. Natl. Acad. Sci. USA *101*, 15184–15189.

Harris, N.L., Jaffe, E.S., Diebold, J., Flandrin, G., Muller-Hermelink, H.K., Vardiman, J., Lister, T.A., and Bloomfield, C.D. (1999). The World Health Organization classification of neoplastic diseases of the hematopoietic and lymphoid tissues. Report of the Clinical Advisory Committee meeting, Airlie House, Virginia, November, 1997. Ann. Oncol. *10*, 1419–1432.

Ji, H., Jiang, H., Ma, W., Johnson, D.S., Myers, R.M., and Wong, W.H. (2008). An integrated software system for analyzing ChIP-chip and ChIP-seq data. Nat. Biotechnol. *26*, 1293–1300.

Jung, N., Dai, B., Gentles, A.J., Majeti, R., and Feinberg, A.P. (2015). An LSC epigenetic signature is largely mutation independent and implicates the HOXA cluster in AML pathogenesis. Nat. Commun. *6*, 8489.

Kawagoe, H., Humphries, R.K., Blair, A., Sutherland, H.J., and Hogge, D.E. (1999). Expression of HOX genes, HOX cofactors, and MLL in phenotypically and functionally defined subpopulations of leukemic and normal human hematopoietic cells. Leukemia *13*, 687–698.

Krejci, O., Wunderlich, M., Geiger, H., Chou, F.S., Schleimer, D., Jansen, M., Andreassen, P.R., and Mulloy, J.C. (2008). p53 signaling in response to increased DNA damage sensitizes AML1-ETO cells to stress-induced death. Blood *111*, 2190–2199.

Kroon, E., Krosl, J., Thorsteinsdottir, U., Baban, S., Buchberg, A.M., and Sauvageau, G. (1998). Hoxa9 transforms primary bone marrow cells through specific collaboration with Meis1a but not Pbx1b. EMBO J. *17*, 3714–3725.

Lengerke, C., and Daley, G.Q. (2012). Caudal genes in blood development and leukemia. Ann. N Y Acad. Sci. *1266*, 47–54.

Licht, J.D. (2001). AML1 and the AML1-ETO fusion protein in the pathogenesis of t(8;21) AML. Oncogene *20*, 5660–5679.

Lo, M.C., Peterson, L.F., Yan, M., Cong, X., Jin, F., Shia, W.J., Matsuura, S., Ahn, E.Y., Komeno, Y., Ly, M., et al. (2012). Combined gene expression and DNA occupancy profiling identifies potential therapeutic targets of t(8;21) AML. Blood *120*, 1473–1484.

Maiques-Diaz, A., Chou, F.S., Wunderlich, M., Gómez-López, G., Jacinto, F.V., Rodriguez-Perales, S., Larrayoz, M.J., Calasanz, M.J., Mulloy, J.C., Cigudosa, J.C., and Alvarez, S. (2012). Chromatin modifications induced by the AML1-ETO fusion protein reversibly silence its genomic targets through AML1 and Sp1 binding motifs. Leukemia *26*, 1329–1337.

Marcucci, G., Geyer, S., Zhao, J., Caroll, A.J., Bucci, D., Vij, R., Blum, W., Pardee, T., Wetzler, M., Stock, W., et al. (2013). Adding the KIT inhibitor dasatinib (DAS) to standard induction and consolidation therapy for newly diagnosed patients (pts) with core binding factor (CBF) acute myeloid leukemia (AML): initial results of the CALGB 10801 (Alliance) Study. Blood *21*, 615a.

Martens, J.H., Brinkman, A.B., Simmer, F., Francoijs, K.J., Nebbioso, A., Ferrara, F., Altucci, L., and Stunnenberg, H.G. (2010). PML-RARalpha/RXR Alters the Epigenetic Landscape in Acute Promyelocytic Leukemia. Cancer Cell *17*, 173–185.

Martens, J.H., Mandoli, A., Simmer, F., Wierenga, B.J., Saeed, S., Singh, A.A., Altucci, L., Vellenga, E., and Stunnenberg, H.G. (2012). ERG and FLI1 binding sites demarcate targets for aberrant epigenetic regulation by AML1-ETO in acute myeloid leukemia. Blood *120*, 4038–4048.

Martin, M. (2011). Cutadapt removes adapter sequences from high-throughput sequencing reads. EMBnet J. *17*, 200.

McGonigle, G.J., Lappin, T.R., and Thompson, A. (2008). Grappling with the HOX network in hematopoiesis and leukemia. Front. Biosci. *13*, 4297–4308.

Moens, C.B., and Selleri, L. (2006). Hox cofactors in vertebrate development. Dev. Biol. *291*, 193–206.

Network, C.G.A.R.; Cancer Genome Atlas Research Network (2013). Genomic and epigenomic landscapes of adult de novo acute myeloid leukemia. N. Engl. J. Med. *368*, 2059–2074.

Patel, P.R., Sun, H., Li, S.Q., Shen, M., Khan, J., Thomas, C.J., and Davis, M.I. (2013). Identification of potent Yes1 kinase inhibitors using a library screening approach. Bioorg. Med. Chem. Lett. *23*, 4398–4403.

Pineault, N., Buske, C., Feuring-Buske, M., Abramovich, C., Rosten, P., Hogge, D.E., Aplan, P.D., and Humphries, R.K. (2003). Induction of acute myeloid leukemia in mice by the human leukemia-specific fusion gene NUP98-HOXD13 in concert with Meis1. Blood *101*, 4529–4538.

Ptasinska, A., Assi, S.A., Mannari, D., James, S.R., Williamson, D., Dunne, J., Hoogenkamp, M., Wu, M., Care, M., McNeill, H., et al. (2012). Depletion of RUNX1/ETO in t(8;21) AML cells leads to genome-wide changes in chromatin structure and transcription factor binding. Leukemia *26*, 1829–1841.

Rawat, V.P., Thoene, S., Naidu, V.M., Arseni, N., Heilmeier, B., Metzeler, K., Petropoulos, K., Deshpande, A., Quintanilla-Martinez, L., Bohlander, S.K., et al. (2008). Overexpression of CDX2 perturbs HOX gene expression in murine progenitors depending on its N-terminal domain and is closely correlated with deregulated HOX gene expression in human acute myeloid leukemia. Blood *111*, 309–319.

Rawat, V.P., Humphries, R.K., and Buske, C. (2012). Beyond Hox: the role of ParaHox genes in normal and malignant hematopoiesis. Blood *120*, 519–527.

Salat, D., Liefke, R., Wiedenmann, J., Borggrefe, T., and Oswald, F. (2008). ETO, but not leukemogenic fusion protein AML1/ETO, augments RBP-Jkappa/SHARP-mediated repression of notch target genes. Mol. Cell. Biol. *28*, 3502–3512.

Schessl, C., Rawat, V.P., Cusan, M., Deshpande, A., Kohl, T.M., Rosten, P.M., Spiekermann, K., Humphries, R.K., Schnittger, S., Kern, W., et al. (2005). The AML1-ETO fusion gene and the FLT3 length mutation collaborate in inducing acute leukemia in mice. J. Clin. Invest. *115*, 2159–2168.

Shen, W.F., Rozenfeld, S., Kwong, A., Köm ves, L.G., Lawrence, H.J., and Largman, C. (1999). HOXA9 forms triple complexes with PBX2 and MEIS1 in myeloid cells. Mol. Cell. Biol. *19*, 3051–3061.

Spencer, D.H., Young, M.A., Lamprecht, T.L., Helton, N.M., Fulton, R., O'Laughlin, M., Fronick, C., Magrini, V., Demeter, R.T., Miller, C.A., et al. (2015). Epigenomic analysis of the HOX gene loci reveals mechanisms that may control canonical expression patterns in AML and normal hematopoietic cells. Leukemia *29*, 1279–1289.

Team, R.C. (2013). R: A Language and Environment for Statistical Computing (R Foundation for Statistical Computing).

Thorsteinsdottir, U., Kroon, E., Jerome, L., Blasi, F., and Sauvageau, G. (2001). Defining roles for HOX and MEIS1 genes in induction of acute myeloid leukemia. Mol. Cell. Biol. *21*, 224–234.

Trapnell, C., Pachter, L., and Salzberg, S.L. (2009). TopHat: discovering splice junctions with RNA-Seq. Bioinformatics *25*, 1105–1111.

Trapnell, C., Williams, B.A., Pertea, G., Mortazavi, A., Kwan, G., van Baren, M.J., Salzberg, S.L., Wold, B.J., and Pachter, L. (2010). Transcript assembly and quantification by RNA-Seq reveals unannotated transcripts and isoform switching during cell differentiation. Nat. Biotechnol. *28*, 511–515.

Wacker, S.A., Alvarado, C., von Wichert, G., Knippschild, U., Wiedenmann, J., Clauss, K., Nienhaus, G.U., Hameister, H., Baumann, B., Borggrefe, T., et al. (2011). RITA, a novel modulator of Notch signalling, acts via nuclear export of RBP-J. EMBO J. *30*, 43–56.

Westendorf, J.J., Yamamoto, C.M., Lenny, N., Downing, J.R., Selsted, M.E., and Hiebert, S.W. (1998). The t(8;21) fusion product, AML-1-ETO, associates with C/EBP-alpha, inhibits C/EBP-alpha-dependent transcription, and blocks granulocytic differentiation. Mol. Cell. Biol. *18*, 322–333.

Yan, M., Kanbe, E., Peterson, L.F., Boyapati, A., Miao, Y., Wang, Y., Chen, I.M., Chen, Z., Rowley, J.D., Willman, C.L., and Zhang, D.E. (2006). A previously unidentified alternatively spliced isoform of t(8;21) transcript promotes leukemogenesis. Nat. Med. *12*, 945–949.